International Journal of Advanced Engineering and Management Research

Vol. 10, No. 06; 2025

ISSN: 2456-3676

Spatio-temporal Analysis of Bushfire Trends in the Itasy Region of Madagascar

HERITAHINA Rambeloson[1,3], RASOLOMANANA Eddy Harilala[1,2,] RANDRIANJA Kanto[1,3]

[1]Doctoral school engineering and geosciences,
University of Antananarivo, BP 566 Ambohitsaina

[2]Polytechnic School of Antananarivo,
University of Antananarivo, BP 566 Ambohitsaina

[3]University of Itasy,
Faliarivo, Soavinandriana Itasy

doi.org/10.51505/ijaemr.2025.1518 URL: http://dx.doi.org/10.51505/ijaemr.2025.1518

Received: Nov 19, 2025 Accepted: Nov 28, 2025 Online Published: Dec 08, 2025

Abstract

The analysis of the spatio-temporal evolution of bushfires in the Itasy region (6,993 km²), Madagascar, over the period 2015–2024, is based on MODISMCD64A1 and VIIRS 375 m data. The results show that 104,354 ha, or 15% of the regional area, burned at least once in ten years. The fires are concentrated in three main hotspots: north of Miarinarivo, southwest of Soavinandriana, and southeast of Arivonimamo. Land use has a strong influence on the dynamics observed: grasslands account for more than 90% of the burned area (84,700 ha), compared to 9,500 ha for cultivated land and less than 200 ha for trees, shrubs, and bare soil combined. Temporal analysis highlights strong seasonality, with a marked peak in September (3,553 ha/month) and a virtual absence of fires between January and April. The years 2018 (15,937 ha), 2016 (14,851 ha), and 2021 (13,660 ha) were the most affected, while 2022 (4,414 ha) was the least active year. The relationship between fire points (VIIRS) and burned areas is highly linear ($R^2 = 0.76$), with each detected fire corresponding to an average of 8.8 ha burned.

Keywords: Itasy Region, Bush fires, MODIS and VIIRS, Burned area, hotspots

1. Introduction

Madagascar is known worldwide as an island of fire, where vegetation fires, especially during the dry season, affect a significant part of the territory (Fernández-García,2024). Pasture fires and slash-and-burn farming are a recurring annual phenomenon : they contribute significantly to the degradation of natural resources and the loss of biodiversity. It is estimated that around 20% of Madagascar's primary forest has been destroyed by fire and shifting cultivation. In this context, the Itasy region (central plateau of Madagascar, covering an area of approximately 6,993 km²) is not spared : its grassy savannas and agricultural areas are regularly subjected to seasonal burning, particularly during the long dry season (April to December) (R. Hanitriniaina, 2017). Local practices associate fires with pastoral and agricultural management (renewal of pastures,

Vol. 10, No. 06; 2025

ISSN: 2456-3676

preparation of land), but the negative impacts (soil erosion, carbon loss, and threats to endemic ecosystems) raise heated debates on the management strategies to be adopted (R. F.H, 2015).

To better understand the scale of the phenomenon and its dynamics, it is crucial to map the burned areas and their evolution over time. Remote sensing technologies have become essential tools for studying and monitoring fire dynamics at different scales, and satellite sensors offer powerful tools : in particular, Sentinel-2 provides high-resolution multispectral images (10–20) (Copernicus, 2024), (S. P. F. et al., 2004).

Entitled “Spatio-temporal analysis of the evolution of bush fires in the Itasy region of Madagascar,” aims first to map the spatial extent and temporal distribution of burned areas at the regional level; then to identify critical periods of fire occurrence and their interannual variability; then to analyze the relationships between fire cycles and the biophysical characteristics of the territory; and finally to quantify the evolution of the affected areas in order to identify significant trends.

Based on these observations, this study tests two hypotheses: those meteorological variations play a decisive role in the scale of fires, and that satellite monitoring of active fires provides a reliable indicator of the intensity of burning episodes. The joint analysis of these hypotheses aims to better understand the interaction between environmental conditions and anthropogenic pressures in bushfire dynamics.

This study is organized into several complementary sections. The first section presents the materials and methods, detailing the data sources, the processing methods applied, and the analytical tools used for spatio-temporal analysis. The second section presents the results obtained, highlighting the mapping of burned areas, the spatio-temporal distribution of bushfires between 2015 and 2024, the quantification and evolution of burned areas, the relationship between burned areas and active fires, and the relationship between weather conditions and burned areas and active fires. The third section offers an interpretation and discussion of the dynamics observed, comparing the results with the hypotheses formulated, regional trends, and existing knowledge in the literature. Finally, the limitations of the study and futurs prospects are discussed, highlighting the main contributions, methodological constraints, and future avenues that could improve the understanding and management of bushfires in the Itasy region.

2. Data and Methods

2.1. Study area

Located in the center of Madagascar's highlands, the Itasy region covers an area of approximately 6,993 km². It borders the Analamanga region to the north, Bongolava to the west, Vakinankaratra to the south, and Amoron'i Mania to the east. The region is characterized by a mosaic landscape of tapia forests, savannas, agricultural areas, and water bodies, with significant agricultural potential and biodiversity (N.&.A, 2017). However, traditional agricultural practices,

Vol. 10, No. 06; 2025

ISSN: 2456-3676

particularly slash-and-burn farming, as well as logging for fuel and charcoal, contribute to the occurrence of bush fires (V. Raharimalala,253p.2007), (C. Baffert,2006.) The varied topography, consisting of hills, plateaus, and valleys, as well as local climatic conditions, characterized by a prolonged dry season and high temperatures, influence the dynamics and spread of bush fires. These combined natural and anthropogenic factors make the Itasy region particularly vulnerable to recurrent fires, warranting an in-depth spatio-temporal analysis to understand the distribution, frequency, and intensity of fires, as well as their impact on ecosystems and human activities (Cream, 2013, p. 182 p.). The following figure shows a map of the region's location.

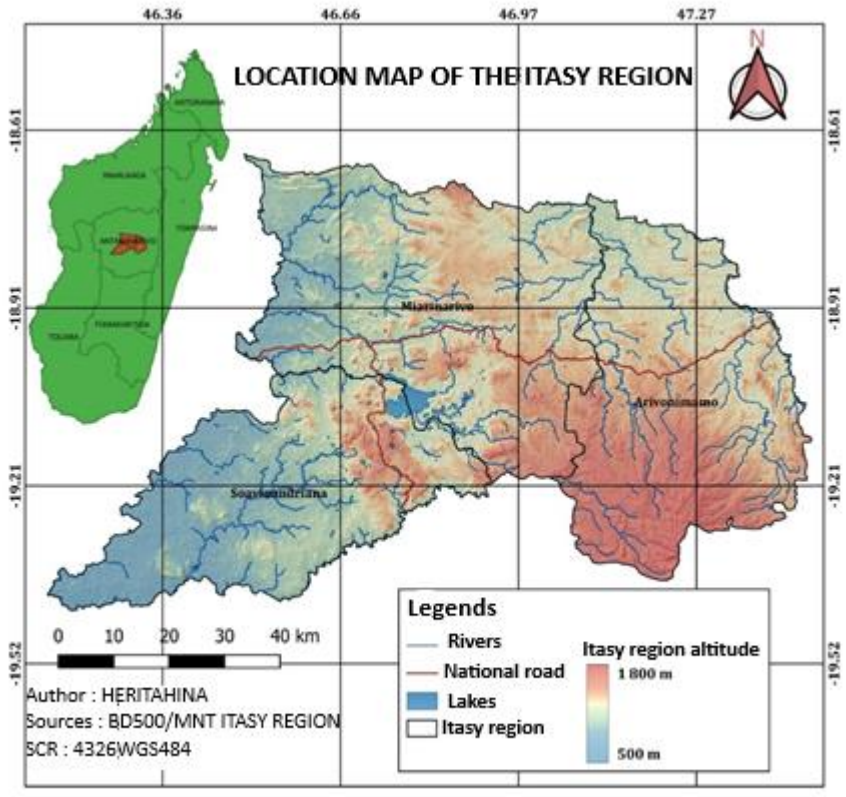

Figure 1. Location map of the Itasy region

2.2. Data set used

The table below compiles all satellite and auxiliary data used for the spatiotemporal analysis of bushfire progression in the Itasy region. It specifies the source, band used, and spatial resolution for each dataset.

Vol. 10, No. 06; 2025

ISSN: 2456-3676

Table 1. Data set used

Data type	Source/product	Band/main variable	Spatial resolution
Total burned area (comparison)	MODIS Burned Area	BurnDate	500 m
Active fire points	VIIRS 375 m Active Fire	Thermal anomalies / active fire	375 m
Land cover	ESA WorldCover 10 m	Land cover class	10 m
Precipitations	CHIRPS v2.0 (Climate Hazards Group InfraRed Precipitation with Station data)	Total precipitation (mm/month)	0,05° (~5 km)
Air temperature	ERA5 – Monthly averaged data on single levels (ECMWF)	Air temperature at 2 m (t2m / mean_2m_air_temperature)	0,25° (~25–30 km)
Relative humidity (RH)	ERA5 – Monthly averaged data on single levels (ECMWF)	Relative humidity near the surface (calculated from t2m and dew point)	0,25° (~25–30 km)
Wind speed	ERA5 – Monthly averaged data on single levels (ECMWF)	Average wind speed at 10 m (u10, v10 / wind speed)	0,25° (~25–30 km)

2.2.1. Land cover – ESA WorldCover

Land cover is described using ESA WorldCover 10 m, version 2021 (v200), developed by the European Space Agency based on Sentinel-1 and Sentinel-2 data. This is a global land cover map with 10 m resolution, available for 2020 and 2021, which distinguishes 11 cover classes, compatible with the FAO classification system (S. H. Collections, 2020.). For this study, the ESA WorldCover layer was downloaded, reprojected, and cropped to the boundaries of the Itasy region, then used to assign a land cover class to each pixel or polygon of burned area. This makes it possible to quantify the total area and annual burned area for each type of environment (savannah, crops, wooded areas, wetlands, etc.). The following table shows the land cover classes according to WorldCover. (L. B. e. al., 2018.)

Vol. 10, No. 06; 2025

ISSN: 2456-3676

Table 2. Land use classification

Code	Class	Color code	Summary description
10	Tree cover	0x006400	Dense tree formations, natural or planted forests
20	Shrubland	0xffbb22	Shrub formations, bushes
30	Grassland	0xffff4c	Natural grasslands, prairies, grassy savannas
40	Cropland	0xf096ff	Cultivated land (rainfed or irrigated)
50	Built-up	0xfa0000	Built-up areas, infrastructure
60	Bare / sparse vegetation	0xb4b4b4	Bare ground or very sparse vegetation
70	Snow and ice	0xf0f0f0	Permanent or seasonal snow and ice
80	Permanent water bodies	0x0064c8	Lakes, rivers, reservoirs, permanent water bodies
90	Herbaceous wetland	0x0096a0	Herbaceous wetlands, marshes
95	Mangroves	0x00cf75	Mangroves (coastal, tropical)
100	Moss and lichen	0xfae6a0	Areas dominated by mosses and lichens

2.2.2. Land use distribution in the Itasy region

Figure (2) below illustrates the surface area by type of land cover in the Itasy region: grasslands account for approximately 52.5%, cultivated land 44.1%, shrub formations 1.1%, permanent water bodies 0.9%, bare soil or sparse vegetation 0.7%, tree cover 0.5%, built-up areas 0.3%, and herbaceous wetlands less than 0.01% of the area.

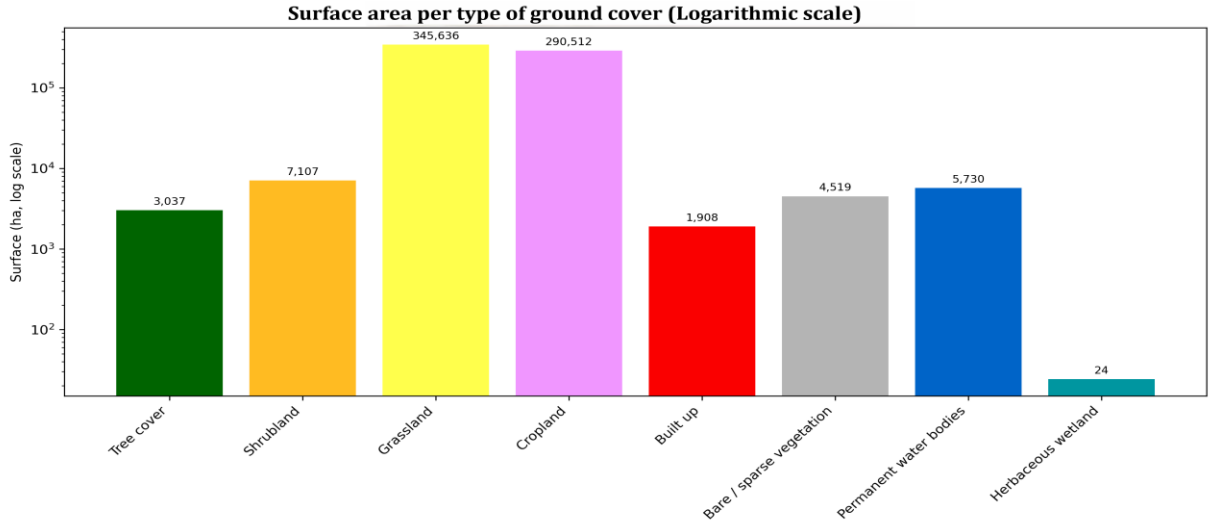

Figure 2. Land cover distribution in the Itasy region

Vol. 10, No. 06; 2025

ISSN: 2456-3676

2.2.3. MODMCD64A1 global burned area product

In this study, MCD64A1 data are obtained via scripts on Google Earth Engine, spatially filtered on the Itasy region, and aggregated temporally by year (and, where applicable, by season). From the BurnDate band, burned pixels are converted into monthly and annual burned area maps, and then the areas are calculated in hectares for the entire region and for each district. [13] [14]

2.2.4. VIIRS Active Fire Points

To characterize the dynamics of fire outbreaks in the Itasy region, the study uses the VIIRS 375m thermal anomalies active fire product. This product is derived from the VIIRS (Visible Infrared Imaging Radiometer Suite) sensor aboard the Suomi NPP and NOAA-20/21 satellites, and provides the location of thermal anomalies/active fires in the form of point pixels with a spatial resolution of 375 m, with a typical revisit of two passes per day (day and night orbits) [15]. VIIRS active fire points are used to complement burned area maps (Sentinel-2 and MODIS MCD64A1): [16] [17]

- They provide very detailed information on the time and location of ignition or passage of the fire front, including for small fires;
- They enable the temporal consistency of burned areas to be verified (presence of fire points near burned polygons on the expected dates);
- They are used to analyze the relationship between the frequency of fire starts and burned area (correlation between the number of VIIRS pixels and burned areas per month/year and by type of cover).

2.2.5 Werther data

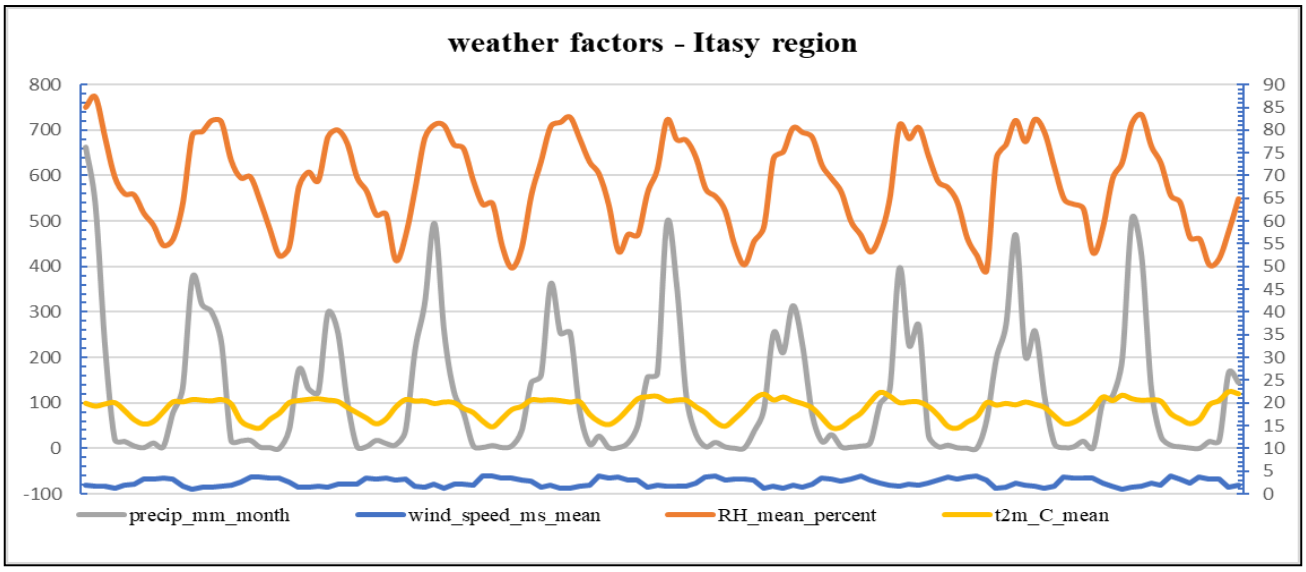

Figure 3. Weather factors in the Itasy region from 2015 to 2024

Vol. 10, No. 06; 2025

ISSN: 2456-3676

Atmospheric conditions were characterized using CHIRPS v2.0 (Climate Hazards Group InfraRed Precipitation with Station data) precipitation data, used as total monthly precipitation at a resolution of 0.05° (~5 km). The air temperature at 2 m, relative humidity near the surface (derived from air temperature and dew point), and average wind speed at 10 m were obtained from ERA5 reanalysis – Monthly averaged data on single levels (ECMWF), with a spatial resolution of 0.25° (25–30 km).

All of these meteorological variables describe the hydro-climatic regime (dryness or moisture of the soil and vegetation) and air circulation conditions, which influence both the outbreak and spread of fires and the dispersion of smoke and pollutants.

2.3. Methodological approach

First, the study area is delimited based on the administrative boundaries of the Itasy region, which serve as a spatial mask for all processing. Within this area,

At the same time, the Google Earth Engine (GEE) platform is also used to exploit various databases such as MODIS fire products and VIIRS data, which are extracted and filtered temporally over the same period in order to provide continuous information on the location and frequency of fires. Next, the ESA WorldCover land cover map is also imported and cut out for the Itasy region to distinguish the main cover classes (savannahs, agricultural areas, wooded areas, water bodies, etc.). All of these layers burned areas and MODIS/VIIRS fire points, land cover are exported to Qgis, where the final spatial and statistical analyses are performed: cross-referencing burned areas with land cover types, mapping the distribution and recurrence of fires, and representing their spatio-temporal evolution at the regional scale.

2.4. Exploratory Data Analysis (EDA)

An exploratory data analysis was performed using descriptive and graphical statistical tools: frequency histograms, box plots, QQ (quantile-quantile) diagrams, and correlation coefficients (r, R^2) to characterize the distribution of fire-related variables and study their relationships**.**

2.4.1. Frequency histogram

The simplest graphical tool is the frequency histogram. This involves automatically dividing the variable's definition interval into k intervals of equal width, then producing a series of bars whose height is proportional to the number associated with the interval.
The number k of intervals is defined arbitrarily but can also be parameterized. A simple rule for defining the correct number of intervals is to use the rule

$$\boldsymbol{k = \log_2(n)} \quad (1)$$

Vol. 10, No. 06; 2025

ISSN: 2456-3676

Our model automatically estimates the two main parameters of the normal distribution (μ the mean, σ the standard deviation) and plots the corresponding density function to assess the closeness between the empirical distribution (histogram) and the theoretical distribution.
The mean is estimated using the empirical mean :

$$\bar{x} = \frac{1}{n}\sum_{i} x_i \quad (2)$$

We use the unbiased estimator of the standard deviation :

$$s = \sqrt{\frac{1}{n-1}\sum_{i}(x_i - \bar{x})^2} \quad (3)$$

2.4.2. Pearson correlation

In order to analyze the linear relationships between the different variables considered (air pollutants and possibly meteorological parameters), a Pearson correlation matrix was calculated. This matrix groups together the correlation coefficients r that exist between all pairs of variables observed in a square table. Pearson's linear correlation coefficient, which can be calculated and understood for two quantitative variables, makes it possible to assess the intensity and direction of the linear relationship between them. [20]
For two variables X and Y, Pearson's correlation coefficient r_XY is defined by :

$$r_{XY} = \frac{\sum_{i=1}^{n}(x_i - \bar{x})(y_i - \bar{y})}{\sqrt{\sum_{i=1}^{n}(x_i - \bar{x})^2}\sqrt{\sum_{i=1}^{n}(y_i - \bar{y})^2}} \quad (4)$$

Where x_i and y_i represent the observed values of variables X and Y, x and y their respective means, and n the number of observations. The coefficients r take values between –1 and +1. A value close to +1 indicates a strong positive linear correlation (the two variables tend to move in the same direction), a value close to –1 indicates a strong negative linear correlation (an increase in one is associated with a decrease in the other), while a value close to 0 suggests the absence of a marked linear relationship.

For this study, Pearson's correlation matrix was established based on the series of monthly averages for each year of the period under consideration. This approach makes it possible to identify pollutants that behave similarly over time, likely due to common emission sources or similar formation mechanisms, and to track the evolution of these relationships from year to year.

The correlation matrices obtained in this way constitute a diagnostic tool for understanding the Pearson correlation matrix R brings together all the coefficients rij between each pair of

Vol. 10, No. 06; 2025

ISSN: 2456-3676

variables (pollutants, meteorological parameters) : signatures of sources and interactions between pollutants in the region studied.

$$R = \begin{pmatrix} 1 & r_{12} & \dots & r_{1p} \\ r_{21} & 1 & \dots & r_{2p} \\ \vdots & \vdots & \ddots & \vdots \\ r_{p1} & r_{p2} & \dots & 1 \end{pmatrix} \quad (5)$$

3. Results

3.1. Temporal analysis of the annual distribution of bushfires between 2015 and 2024

Figure 4 shows that bushfires do not affect the area uniformly. Over the study period, the burned area reached 1,043.54 km², or about 15% of the total area of the Itasy region. This area corresponds to all pixels burned at least once over the ten years, highlighting the areas that have been repeatedly affected by fires.

Spatially, three large areas of burned land stand out clearly. The first is located in the north of the region, above Miarinarivo, where the red spots are very dense and continuous: this is a real hotspot for recurring fires. The second appears in the southwestern tip, in the district of Soavinandriana, where fires are concentrated on slopes and open plateaus. The last is visible in the southeast of the district of Arivonimamo.

Conversely, the eastern part and some central areas have far fewer burned areas, suggesting either lower fire pressure or topographical and land use conditions that are less conducive to the spread of fires. The integration of land cover data makes it possible to link these burning anomalies to land cover types. The map shows that the vast majority of burned areas overlap with areas colored yellow, which are natural grasslands or pastures, and pink, which correspond to cultivated areas, while tree cover remains relatively unaffected. This recurrence of fire in the same landscape units reflects a marked spatio-temporal dynamic: during the years 2015–2024, it is mainly the same areas of grassland and crops that are set on fire, while other parts of the region remain marginally affected.

Vol. 10, No. 06; 2025

ISSN: 2456-3676

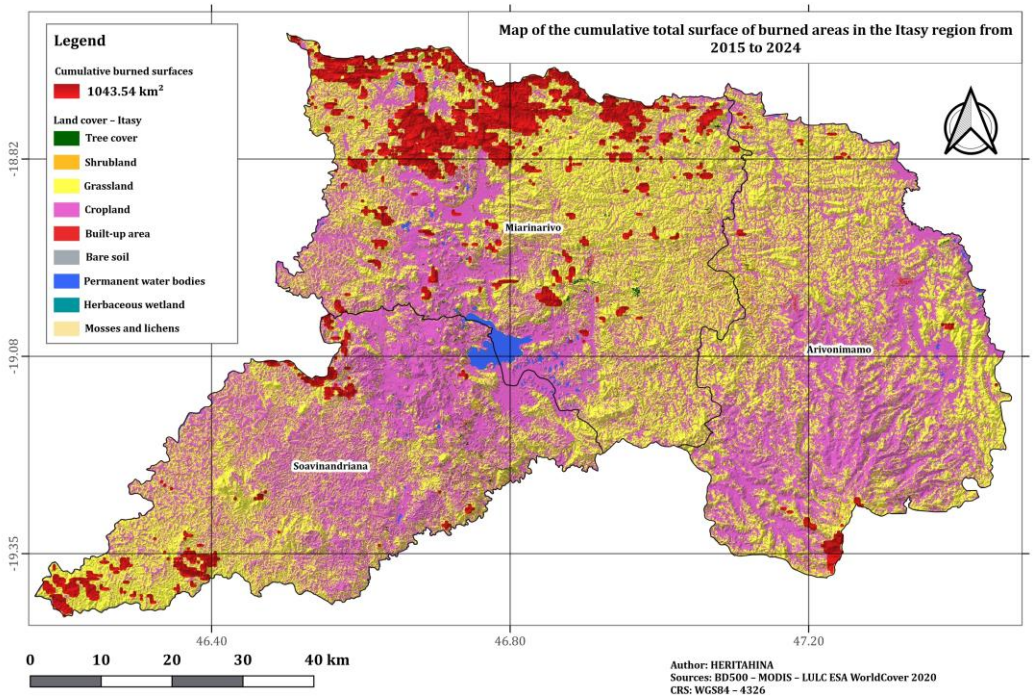

Figure 4. Map of the total cumulative area burned in the Itasy region between 2015 and 2024

To better appreciate this distribution of burned areas, the following histogram shows the surface area of burned areas in relation to land use.

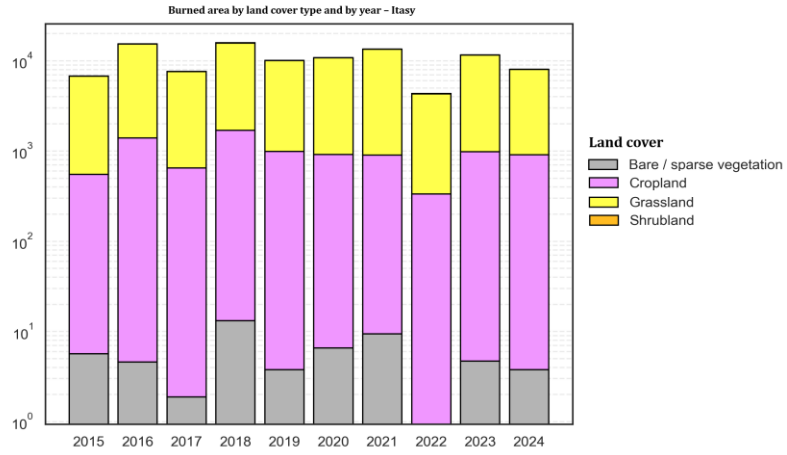

Figure 5. Histogram showing the distribution of burned areas according to land use

Vol. 10, No. 06; 2025

ISSN: 2456-3676

The breakdown by land use reveals that, in all the years analyzed, grasslands and croplands are the two main categories affected by bushfires. Grasslands alone account for more than 90% of the burned land. The following table details the distribution of burned areas by land use class.

Table 3. Distribution of burned areas by land use class

Year	Bare land or sparse vegetation (ha)	Cultivated land (ha)	Grassland (ha)	Shrub formation (ha)	Tree cover (ha)
2015	5.952	585.221	6 406.203	14.093	0.827
2016	4.588	1 390.388	13 446.076	4.706	5.704
2017	2.883	667.100	6 996.704	2.883	0.942
2018	13.183	1 689.008	4 201.961	25.044	8.460
2019	3.967	993.174	9 194.724	2.925	1.942
2020	6.891	929.485	9 895.582	2.826	3.767
2021	9.414	898.981	12 742.043	5.650	3.764
2022	1.942	393.494	3 991.987	25.342	1.882
2023	4.707	991.036	10 671.989	1.884	2.825
2024	3.967	962.300	7 125.003	5.649	2.926

It is estimated that nearly 84,700 ha of grassland have been ravaged by fire, while cultivated land has been affected over an area of approximately 9,500 ha. Tree cover, shrub formations, and sparse vegetation cover a total area of just over 180 ha.

From one year to the next, grassland remains the most affected land type, with burned areas varying between approximately 4,000 and 7,000 hectares (2015, 2017, 2018, 2022, 2024) and more than 9,000 to 13,000 ha in some years (2016, 2019, 2020, 2021, 2023). The years 2016 and 2021 stand out as particularly critical, with more than 13,000 ha of grassland burned, while 2022 was a significantly less active year with around 4,000 ha. Cultivated land follows the same pattern but with lower values, generally in the range of 400 to 1,700 ha per year. The other categories (bare soil, shrubland, wooded areas) remain very marginal, rarely exceeding a few dozen hectares per year.

3.2. Quantification and evolution of burned areas from 2015 to 2024

The figure below shows the monthly evolution, the total burned area, and the average seasonal cycles of burned areas.

Vol. 10, No. 06; 2025

ISSN: 2456-3676

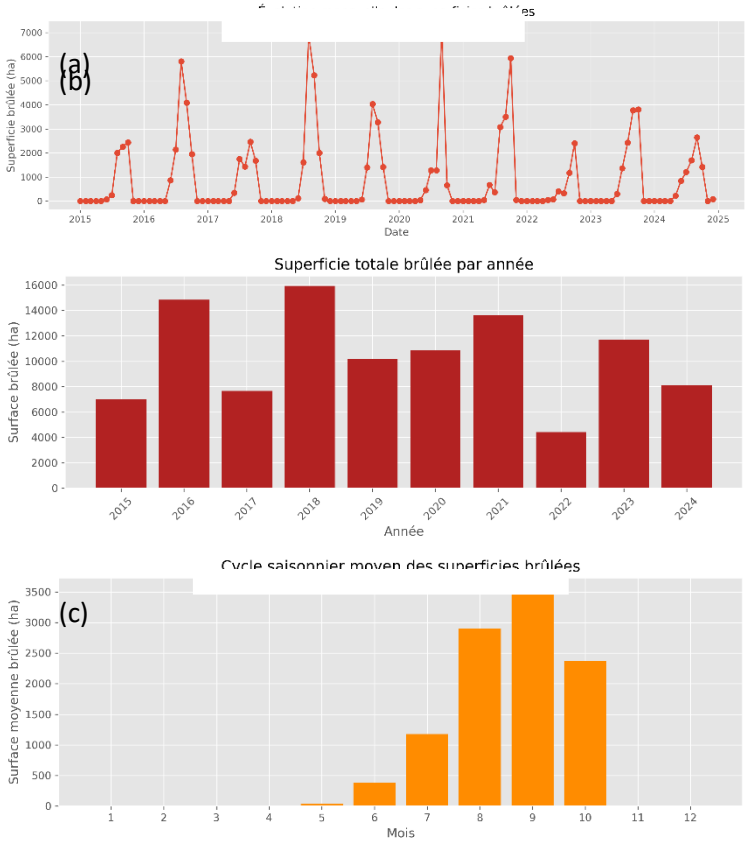

Figure 6. Quantification and evolution of burned areas

During the period 2015-2024, the total area burned amounted to 104,354 ha, or almost 15% of the region's area, which was affected at least once by bushfires, equivalent to an average of 870 ha per month. The maximum monthly value was recorded in September 2020 with 7,125 ha burned, which is more than eight times the monthly average during this period. (Figure 5a)

The annual trend (Figure 5b) shows significant interannual variability rather than a linear trend. The years 2018 (15,937 ha), 2016 (14,851 ha), and 2021 (13,660 ha) were the most affected, while 2022 had the smallest burned area (4,414 ha). Years of high activity correspond to more pronounced dry seasons or an intensification of agro-pastoral burning practices, while 2022 could correspond to a wetter climate or more effective fire control. At the national level, several studies show that fire intensity increases during particularly dry and hot years, and that climate change tends to lengthen the fire season. [19]

The monthly graph (Figure 5c) reveals a very pronounced seasonal cycle: the areas burned are almost zero from January to April, and begin to increase in June–July, then reach a maximum between August and October, with an average peak in September (approximately 3,553

Vol. 10, No. 06; 2025

ISSN: 2456-3676

ha/month) followed by August (2,896 ha) and October (2,370 ha). This concentration of fires at the end of the dry season corresponds to the fire regime observed throughout Madagascar, where the fire season generally begins in early August and lasts for about 15 weeks, with a peak in September–October. [20] These results confirm that, in the Itasy region, bush fires are a highly seasonal phenomenon, closely linked to the climatic conditions of the dry season and to the practice of burning for agriculture and grazing.

3.3. Relationship between burned areas and active fires

In order to assess the extent to which the intensity of fire activity detected by satellite actually translates into burned areas, we analyzed the relationship between the number of active fires (VIIRS) and burned areas (MODIS MCD64A1) on a monthly basis in the Itasy region. This approach allows us to test the consistency between active fire detection products and burned area maps, and to assess the ability of the former to serve as an indicator of the true extent of bush fires. Figure (6) below shows the relationship between burned areas and the number of active fires.

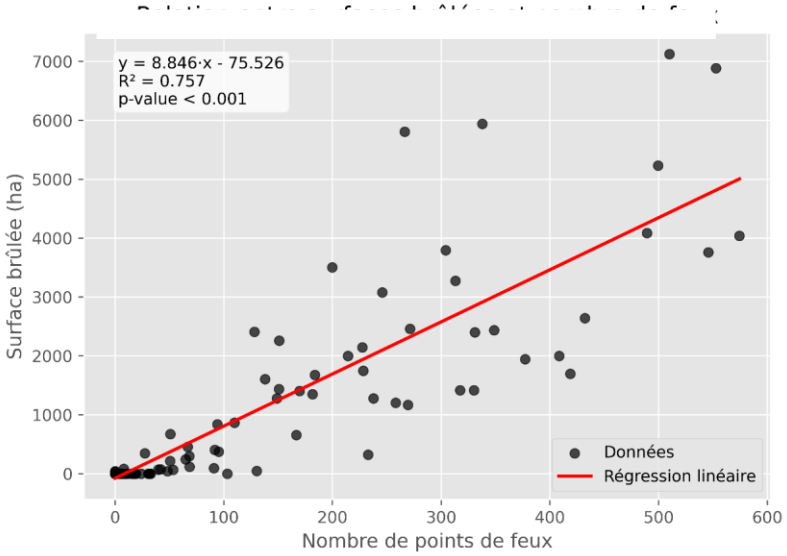

Figure 6. Relationship between burned area and number of active fires

Over all the months studied, the scatter plot shows a linear relationship between the number of fire points and the area burned: as the number of active fires detected increases, the monthly area burned tends to be higher. The estimated regression line is :

$$burned_{area} = 8.846 \times fire_{points} - 75.526$$

Within the range of observed values, this means that an additional fire point is associated with an average of approximately 8.8 ha more burned area.

Vol. 10, No. 06; 2025

ISSN: 2456-3676

The coefficient of determination $R^2 = 0.757$ indicates that approximately 76% of the monthly variability in burned area is explained by the number of fire points. This value reflects a strong statistical relationship: the number of active fires is a good predictor of the extent of burned areas across the region. The remaining 24% of variability is likely related to other factors not included, such as instantaneous weather conditions, fuel type, topography, fire duration, etc.

Finally, the $p - value < 0{,}0001$ shows that the regression slope is very significantly different from zero: the probability of obtaining such a marked relationship by chance alone, in the absence of a real link between fire points and burned area, is less than 0.1%. It can therefore be deduced that the increase in burned areas is strongly linked to an increase in the number of active fires in the Itasy region during the period analyzed.

3.4 Relationship between weather factors explaining burned areas and active fires

This section analyzes the close relationship between bushfire indicators (burned areas and number of fire points) and key weather factors. This relationship makes it possible to measure the strength and direction of linear relationships between different variables in order to identify interactions between environmental conditions conducive to the ignition and spread of fires.

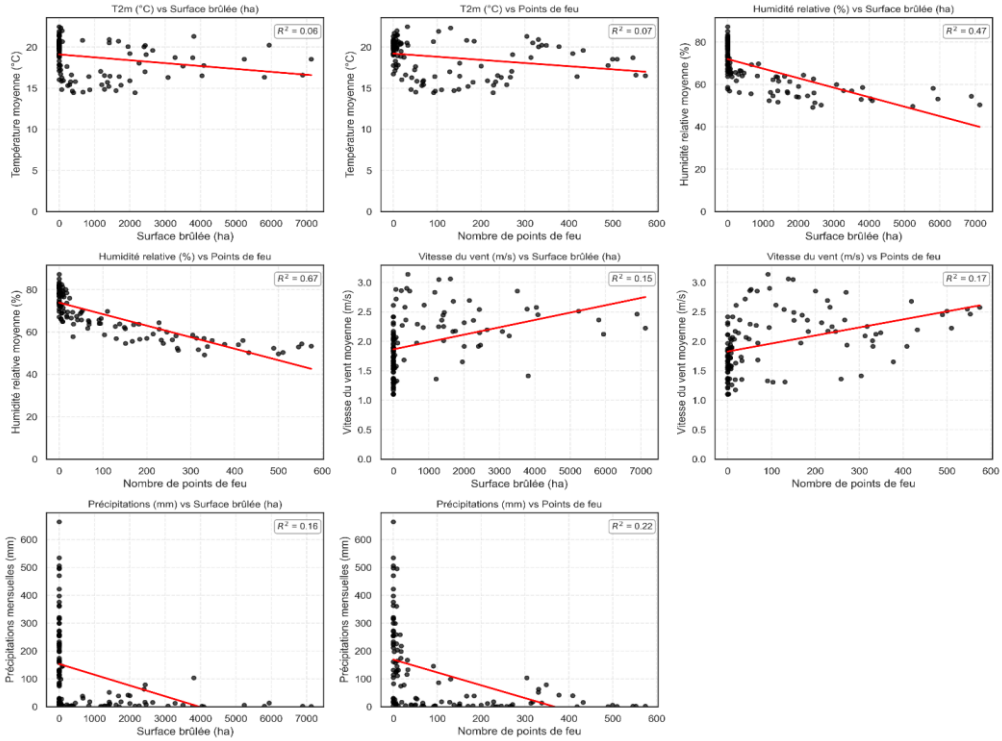

Figure 7. Relationship between meteorological factors and bushfire indicators

Vol. 10, No. 06; 2025

ISSN: 2456-3676

This figure shows the links between meteorological factors and forest fires. At first glance, the diagram indicates that bushfire indicators are mainly influenced by low humidity (low moisture content, lack of rain), and that wind makes matters worse, while temperature is less important.

The average monthly temperature has no real impact. The links between temperature and the area burned ($R^2 = 0.06$) and the number of fire points ($R^2 = 0.07$) are slightly negative, but do not explain much. This means that fire activity does not change significantly with air temperature.

However, relative humidity appears to be the key factor. The negative slope and high figures ($R^2 = 0.47$ for burned areas and $R^2 = 0.67$ for the number of fire points) show a strong inverse relationship. The driest months are always linked to the largest burned areas and the highest number of fires.

Precipitation and wind speed play a moderate role. Monthly rainfall is negatively linked to fires, with R^2 values of around 0.16 for burned areas and 0.22 for the number of fire points. Rainy months have fewer fires, but the proportion explained remains moderate. This suggests that rainfall alone is not enough to determine whether the terrain is dry or not.

Finally, wind speed is positively correlated with both fire indicators ($R^2 = 0.15$ for burned area and 0.17 for fire starts). Strong winds help fires spread and slightly increase their size and number, but their influence is less significant than that of air dryness.

4. Discussion

4.1. Spatiotemporal dynamics

The Itasy region has a clearly differentiated structure in terms of fire dynamics, with a spatial distribution of fires dominated by three recurring hotspots located around Miarinarivo, Soavinandriana, and Arivonimamo. This fire geography essentially reflects land use and agricultural practices, with grasslands and cultivated land accounting for the vast majority of burned areas, while wooded areas and wetter terrain remain marginally affected. The recurrence of burning in the same areas reflects persistent local cycles, rooted in production patterns and landscape configurations that favor the spread of fire. In terms of timing, the strong seasonality with a systematic peak at the end of the dry season highlights the phenomenon's dependence on climatic conditions, while interannual variability, marked in particular by the peaks of 2016, 2018, and 2021 and the sharp decline in 2022, reflects the link between drought and the intensity of fire use.

These dynamics have significant ecological and socio-economic implications, particularly in terms of soil degradation, increased risks to rural infrastructure, and carbon emissions. They justify the implementation of targeted interventions in critical areas, combining regulation and supervision of practices, physical prevention measures, community mobilization, and agroecological incentives. Despite the substantial contribution of remote sensing, several

Vol. 10, No. 06; 2025

ISSN: 2456-3676

uncertainties remain regarding the precise attribution of causes, the severity of fires, and the understanding of socio-territorial determinants, which calls for further investigation combining detailed climate analyses, field surveys, and predictive modeling. All of these elements confirm that fire regimes in Itasy are the result of a combination of environmental constraints, human practices, and landscape dynamics, requiring integrated and territorially differentiated management strategies.

4.2. Explanatory factors

In line with our initial hypothesis that meteorological factors, and atmospheric dryness in particular, play a decisive role in the spread of bushfires, the results show that fire dynamics in the Itasy region are largely controlled by relative humidity, which determines the flammability of plant fuels. Monthly analyses confirm a clear hierarchy among climate variables: average temperature has a marginal influence (R^2 0.06–0.07), while relative humidity appears to be the main determinant of fire activity, with strong inverse correlations (R^2 0.47 for burned areas and 0.67 for active fires), indicating that periods of maximum drought systematically correspond to the most significant spread of fires. Precipitation and wind speed play an intermediate role (R^2 0.15–0.22): rain reduces the drying of biomass, while wind can increase local spread, but their influence remains secondary to air dryness.

In parallel, our second hypothesis stating that the number of active fires is a reliable indicator of burned areas is fully validated: each hotspot detected by VIIRS corresponds on average to 8.8 ha burned, and the linear relationship explains nearly 76% of the monthly dynamics. This shows that the intensity of ignitions, mostly of anthropogenic origin, acts as the triggering factor for the propagation potential driven by atmospheric conditions. This coherence between meteorological data and satellite signals provides a robust explanatory basis, while also requiring a critical reading: certain fine scale factors fuel structure, microrelief, diversity of burning practices remain beyond the scope of regional models but may locally influence propagation trajectories. Nevertheless, this limitation does not diminish the significance of our results; rather, it highlights that the combination of drought and active ignitions constitutes the most relevant framework for understanding and anticipating fire dynamics in Itasy, and it directly guides management strategies toward a coordinated approach combining climate forecasting, controlled burning supervision, and near realtime satellite monitoring.

4.3. Limitations and perspectives

Satellite products (MODIS ~500 m, VIIRS ~375 m) provide robust regional coverage but can underestimate small fires or aggregate disjoint burned areas, leading to an approximate estimate of the burned area. Detection also depends on orbital passes, day or night, and can be influenced by cloud cover or vegetation density. Meteorological data, based on monthly averages, simplify actual climatic variations and do not account for intra-monthly fluctuations that are sometimes critical for fire ignition and spread. These points highlight that, while providing a solid synthesis

Vol. 10, No. 06; 2025

ISSN: 2456-3676

at the regional scale, analyses could benefit from additional data to capture local heterogeneities and refine the understanding of fire dynamics.

To deepen understanding and improve management, several avenues can be explored. From a research perspective, combining MODIS/VIIRS data with other sensors offering higher spatial resolution, such as Sentinel-2 and PlanetScope, would allow for a better characterization of low-intensity fires and the detailed mapping of burned areas. Integrating local climate models (to predict periods of severe drought) and socio-economic data (agricultural practices, population density) would enrich the analysis of fire determinants. In terms of methodology, developing forecasting models that use the number of active fires as a predictor (given the high R^2 obtained) could provide rapid estimates of areas at risk during the dry season.

From a land management perspective, awareness and training campaigns on controlled burning should be intensified at the end of the dry season, emphasizing the exacerbated impact of drought (low humidity) on the spread of fires. It would also be beneficial to improve near real-time aerial and satellite surveillance during the critical season to quickly alert fire services.

5. Conclusion

This study examined in detail how bushfires evolved in the Itasy region between 2015 and 2024, using a combination of several satellite data sources (Sentinel-2, MODIS MCD64A1, VIIRS 375 m) and detailed statistical analyses. The results show that nearly 104,354 hectares, or 15% of the region, were affected by fires at least once in ten years, revealing the scale of the phenomenon and its persistence over time. Three areas emerged as the main hotspots of burning, located in grasslands and agricultural lands, clearly reflecting local agro-pastoral practices. Conversely, wooded and shrubby areas were rarely affected, indicating a high degree of fire selectivity based on habitat type.

In terms of timing, fires follow a very pronounced seasonal pattern, with a recurring peak between August and October, a period during which vegetation is particularly dry. The years 2016, 2018, and 2021 stand out for more intense fire activity, while 2022 appears to have been significantly less affected. Analysis of environmental factors shows that relative humidity plays a central role : when the air is dry, fires spread much more easily than under the influence of temperature, rain, or wind. Furthermore, the strong statistical correlation between active fires detected by VIIRS and the areas actually burned confirms the value of this data for operational and near real-time fire monitoring.

However, despite the quality of the methods used, some limitations remain, notably related to the sometimes insufficient resolution of MODIS/VIIRS data, the use of monthly meteorological averages, and the lack of socio-economic information on fire-setting practices. These limitations open avenues for future research based on higher-resolution images, more precise local climate models, or field investigations to better understand the human dynamics underlying these fires.

Vol. 10, No. 06; 2025

ISSN: 2456-3676

This study shows that bushfires in Itasy result from a close combination of environmental drought and human activity. It highlights the need for integrated management based on climate forecasting, controlled burning, satellite monitoring, and raising awareness among local communities. The results thus provide a solid foundation for guiding public policy decisions and strengthening prevention strategies, in a context where environmental and socio-economic challenges are becoming increasingly urgent.

Acknowledgments

This study benefited greatly from the guidance and scientific expertise provided throughout its development. Insightful feedback, methodological advice, and continuous encouragement significantly strengthened the quality and rigor of the work.
I also extend my gratitude to all those who contributed through discussions, technical assistance, or data processing support, whose efforts were invaluable at various stages of the study.

References

V. F. M. K. Fernández-García, *Madagascar's burned area from Sentinel-2 imagery* (2016–2022), C.A, 2024.

R. Hanitriniaina, *Analyse de la mise en œuvre des strategies*, 2017.

R. F.H., *Analyse spatio-temporelle de la dynamique des feux de végétation*, 2015.

Copernicus, *S2 Mission- Overview of Sentinel-2 Mission*, 2024.

S. P. F. e. al., *Remote sensing of vegetation fires and*, 2004.

N. &. A. International, *Diagnostic des plantations forestières du projet MAHAVOTRA, Région Itasy, Madagascar*, 2017.

V. RAHARIMALALA, *Situation des principaux indicateurs environnementaux à Madagascar. In : Ministère de l'Environnement, de l'Écologie et des Forêts, Rapport sur l'État de l'Environnement de Madagascar, Antananarivo*, 2007, p. 253 p.

C. BAFFERT, *La déforestation à Madagascar*., Mongabay, 2006.

CREAM, *Monographie de la Région Itasy., Antananarivo: Centre de Recherches, d'Études et d'Appui à l'Analyse Économique à Madagascar, 2013, p. 182 p*.

E. W. cover, *Global land cover product at 10m resolution for 2021 based on Sentine-1 and 2 data*, 2021, p. https://worldcover2021.esa.int/.

S. H. Collections, *WorldCover*, 2020.

L. B. e. al., *The Collection 6 MODIS burned area mapping algorithm and product, vol. 217, Remote Sensing of Environment*, 2018.

L. G. (NASA), *Collection 6.1 MODIS Burned Area Product User's Guide*, 2021.

W. W. e. a. Louis Giglio, *VIIRS (and Landsat-class) - Active Fire Data Products*, 2016.

N. FIRMS, VIIRS I-Band 375 m *Active Fire Data*, 2018.

K. e. a. Coskuner, *Assessing the performance of MODIS and VIIRS active fire/hotspot products in wildfire detection*, vol. 15, 2022, p. 345–354.

J. C. J. H. Y. &. C. I. Benesty, *Pearson correlation coefficient. In: Noise reduction in speech processing, Springer, Berlin, Heidelberg*, 2009, p. p. 1–4..

Vol. 10, No. 06; 2025

ISSN: 2456-3676

P. A. a. C. Reid, *Madagascar on Fire… climate change the arsonist?*, 2025.

T. &. L. S. M. Frappier-Brinton, *The burning island: Spatiotemporal patterns of fire occurrence in Madagascar.*, éd., Vols. PLOS ONE, 2022.

U. -L. Missions, *Landsat Normalized Difference Vegetation Index*.

B. K. E. S. C. M. J. Estes, *Factors influencing fire severity under moderate burning conditions in the Klamath Mountains, northern California*, USA., vol. 8(5), Ecosphere, 2017.

NPS (National Park Service), *Wildland Fire Behavior: Topography*, 2017.